

Review

Challenges and Perspectives for Biosensing of Bioaerosol Containing Pathogenic Microorganisms

Meixuan Li, Lei Wang [†], Wuzhen Qi, Yuanjie Liu  and Jianhan Lin ^{*} 

Key Laboratory of Agricultural Information Acquisition Technology, Ministry of Agriculture and Rural Affairs, China Agricultural University, Beijing 100083, China; 2018308130117@cau.edu.cn (M.L.); wanglei123@cau.edu.cn (L.W.); wuzhen.qi@cau.edu.cn (W.Q.); yjliu@cau.edu.cn (Y.L.)

* Correspondence: jianhan@cau.edu.cn

[†] Co-first author: This author contributes equally to the first author.

Abstract: As an important route for disease transmission, bioaerosols have received increasing attention. In the past decades, many efforts were made to facilitate the development of bioaerosol monitoring; however, there are still some important challenges in bioaerosol collection and detection. Thus, recent advances in bioaerosol collection (such as sedimentation, filtration, centrifugation, impaction, impingement, and microfluidics) and detection methods (such as culture, molecular biological assay, and immunological assay) were summarized in this review. Besides, the important challenges and perspectives for bioaerosol biosensing were also discussed.

Keywords: bioaerosol; collection; biosensing; microfluidic chip; pathogenic microorganisms



Citation: Li, M.; Wang, L.; Qi, W.; Liu, Y.; Lin, J. Challenges and Perspectives for Biosensing of Bioaerosol Containing Pathogenic Microorganisms. *Micromachines* **2021**, *12*, 798. <https://doi.org/10.3390/mi12070798>

Academic Editor: Yi Peng

Received: 12 June 2021

Accepted: 4 July 2021

Published: 5 July 2021

Publisher's Note: MDPI stays neutral with regard to jurisdictional claims in published maps and institutional affiliations.



Copyright: © 2021 by the authors. Licensee MDPI, Basel, Switzerland. This article is an open access article distributed under the terms and conditions of the Creative Commons Attribution (CC BY) license (<https://creativecommons.org/licenses/by/4.0/>).

1. Introduction

Bioaerosols within the diameter of 100 μm mainly refer to bacteria, viruses, fungi, and some microbial fragments suspended in the air [1–3]. The size of bioaerosols containing fungi, bacteria, and viruses generally range from 1 to 30 μm , from 0.25 to 8 μm and less than 0.3 μm , respectively [4,5]. According to the report from the World Health Organization, lower respiratory infections remained the world's most deadly communicable disease and were ranked as the 4th leading cause of death, resulting in 2.6 million deaths in 2019 [6]. Severe Acute Respiratory Syndrome (SARS) in 2003 [7,8], H1N1 Influenza in 2009 [9,10], Middle East Respiratory Syndrome in 2013 [11–13], and Coronavirus (COVID-19) pandemic in 2019 [14–16] could also be spread through bioaerosols, which pose a great threat to global public health. Therefore, it is vital to monitor bioaerosols containing microorganism pathogens for prevention and control of the outbreaks of epidemic airborne diseases.

The collection and detection of bioaerosols are two important procedures for bioaerosol monitoring. Since several good review articles have summarized bioaerosol collection [1–4,17,18] and bioaerosol detection [1,19–21], the follow-up and emerging studies on bioaerosol collection and detection are summarized and discussed in this review to broaden the sight of the scientists and promote the studies on bioaerosol monitoring.

2. Bioaerosol Collection

The collection of bioaerosols is the essential prerequisite for pathogen detection, which is also an important part of bioaerosol monitoring. The bioaerosol collection methods basically rely on the physical properties of bioaerosols, such as weight and size. Currently, available bioaerosol collection methods mainly include sedimentation, filtration, centrifugation, impaction, impingement, and microfluidic chips. All these methods are able to collect bioaerosols, but their performance is susceptible to factors, such as temperature, humidity, airflow, etc. Some newly improved studies on bioaerosol collection methods are updated and compared in this section.

2.1. Sedimentation

Natural sedimentation was once used for bioaerosol collection since it was first proposed by Koch in 1881 using nutrient agar plates to collect the settling bioaerosols containing bacteria due to their own gravity, followed by incubation of the bacteria and enumeration of the colonies. This sedimentation was demonstrated with low efficiency by Sui et al. [22] by first using the aerosol generator to nebulize the bacterial suspension at the concentration of 10^4 CFU/mL for mimicking bioaerosols containing bacteria in a 125-L tank, then placing the Luria-Bertani (LB) agar plates in the tank for 20 min, and finally incubating the plate at 37 °C for 24 h to count the number of the colonies. The results showed that only 26 bacterial cells were collected by this natural sedimentation. Although the sedimentation method has shown its merits of low cost, easy operation, and little impact on microbial activity, its practical applicability is greatly limited due to (1) low collection efficiency, especially for bioaerosols with smaller size ($<1 \mu\text{m}$), (2) strong external interferences, especially for complex environments, and (3) more importantly, increasing microbial risk resulting from cultured pathogenic microorganisms.

Recently, sedimentation is also used with electrostatic adsorption to collect the bioaerosols [23–25]. An external electric field is often applied to attract or repel the charged bioaerosols due to the electrostatic effect, thus resulting in the collection of bioaerosols onto agar, liquid, and solid surfaces [26–29]. In theory, bioaerosols with more electric charges are more easily subject to electrostatic sedimentation, and vice versa. The corona discharge was reported to enable the bioaerosols to carry more electric charges, thus making the bioaerosols more easily collected onto the electrodes [30–34]. An interesting electrostatic sedimentation method for the collection of the bioaerosols was shown in Figure 1. A commercially available miniature air ionizer was used to generate electrical charges through corona discharge. When the bioaerosols arrived at the ionization region, they were charged by colliding with the charges and captured by an electrostatic precipitator. The results showed that the collection efficiency of the device in collecting biological particles of $1 \mu\text{m}$ was as high as $84 \pm 7\%$ [35]. The electrostatic sedimentation has shown a higher collection efficiency due to electrostatic attraction of charged bioaerosols, a better universality due to less impact from particle size, and a stronger collection capacity due to continuous-flow capture of bioaerosols. However, the activity of pathogenic microorganisms in the bioaerosols might be greatly reduced due to the electric charges, and the extremely high voltage for corona discharge is still a potential risk for practical applications.

2.2. Filtration

Filtration is frequently used to collect the bioaerosols [36,37]. The filters are often made of different materials, including polycarbonate, cellulose ester, polytetrafluoroethylene, polyvinyl chloride, nylon, gelatin, glass fiber, alumina nanofiber, and others [3,17,38]. According to the physical structure, the filters could be divided into three categories: fibrous filter, porous membrane filter, and capillary pore filter. A typical example was reported by Biswas et al. and shown in Figure 2A. A gelatin filter and a glass fiber filter were compared for physical collection of the bioaerosols containing influenza viruses. The atomizer was first used to aerosolize the viral solution to form the bioaerosols containing viruses. After they were drawn through the filter, the bioaerosols were collected on the dry film of the filter due to diffusion, interception, and impaction. Finally, the collected bioaerosols were determined using viral isolation and real-time Reverse Transcription-Polymerase chain reaction (RT-PCR). The results showed that both of the gelatin and glass fiber filters had a high collection efficiency. Compared to the glass filter, the gelatin filter had a lower stability but a higher virus recovery. However, only high concentrations of bioaerosols containing viruses could lead to positive results [39]. Another interesting example was reported by Jung et al. and shown in Figure 2B. The bioaerosols containing bacteria were first negatively charged through collision with negative ions generated by the ionizer at a constant voltage of -10 kV . When the charged bioaerosols passed through

the positively charged polyester/aluminum filters, they were captured in the filters due to electrostatic interactions. The results showed that this filter had a very high collection efficiency ($\sim 99.99\%$) for the bioaerosols with a geometric mean diameter of $\sim 0.89 \mu\text{m}$ [40]. At present, many commercial filters were available, such as the button bioaerosol sampler from SKC (Covington, NC, USA) and the GSP bioaerosol sampler from BGI (Waltham, MA, USA) [2].

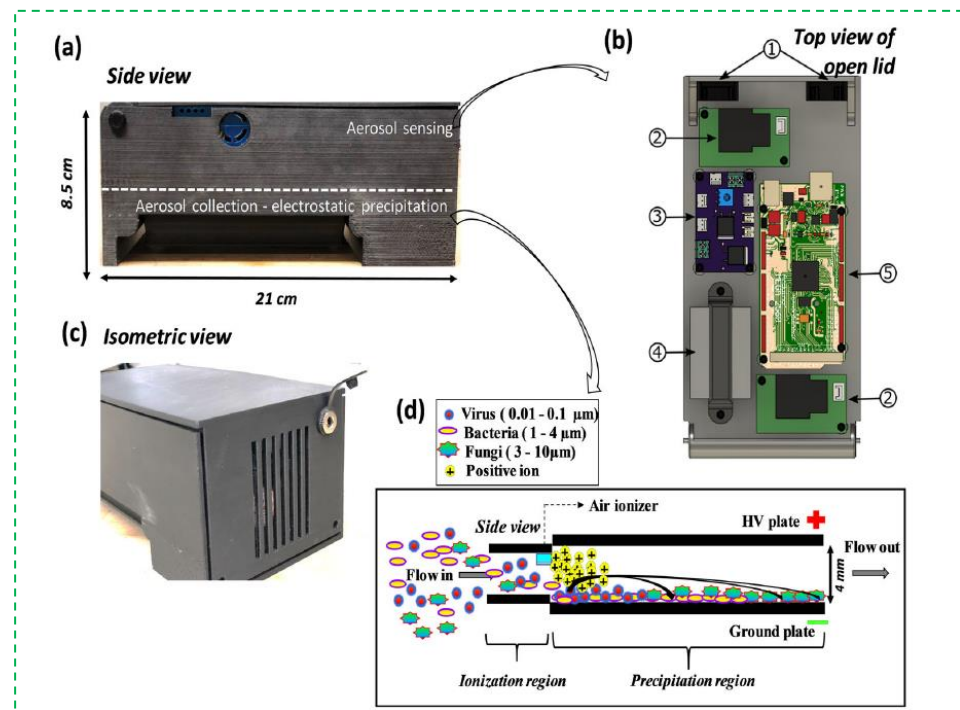


Figure 1. The electrostatic sedimentation for collection of bacterial bioaerosols. (a) side view of the device; (b) the aerosol sensing components; (c) isometric view of the device; (d) schematic representation of the side view of the electrostatic precipitator situated at the bottom of the device. Reprinted with permission from ref. [35]. Copyright 2021 Taylor & Francis.

The filtration method has shown its merits of small size, low cost, and easy operation. However, it still has some limitations, such as (1) uncontrollable collection size due to uneven pore size of the filters, (2) inaccurate collection efficiency due to incomplete elution of the bioaerosols and easy blocking of the filters, and (3) low collection velocity due to the fragility of the filters. Besides, the complexity of the air environment and the heterogeneity of bioaerosol size also make the sampling difficult.

2.3. Centrifugation

The centrifugation method is also reported to collect the bioaerosols. In general, the bioaerosols are injected into a special-structured chamber to form the swirling air, resulting in the centrifugation of the bioaerosols into the collection wall or liquid due to their different mass [41–45]. A typical example was reported by Jung et al. and shown in Figure 3. A stable thin liquid film was first formed in a conical cyclone chamber due to the centrifugation and gravity. When the bioaerosols were injected into the chamber, a helical cyclone was then formed, and the bioaerosols were finally centrifuged into the liquid film, which was drained out from the bottom, while the clean air was drained out from the top. The results showed that this centrifugation method could collect $>95\%$ of the particles with a diameter of $>0.5 \mu\text{m}$ and the bioaerosols containing *Staphylococcus epidermidis* and *Micrococcus luteus* [46]. Combined with the adenosine triphosphate-bioluminescence technique, this method was able to detect the bioaerosols containing *E.coli* cells as low as $130 \text{ CFU}/\text{m}^3$ [47].

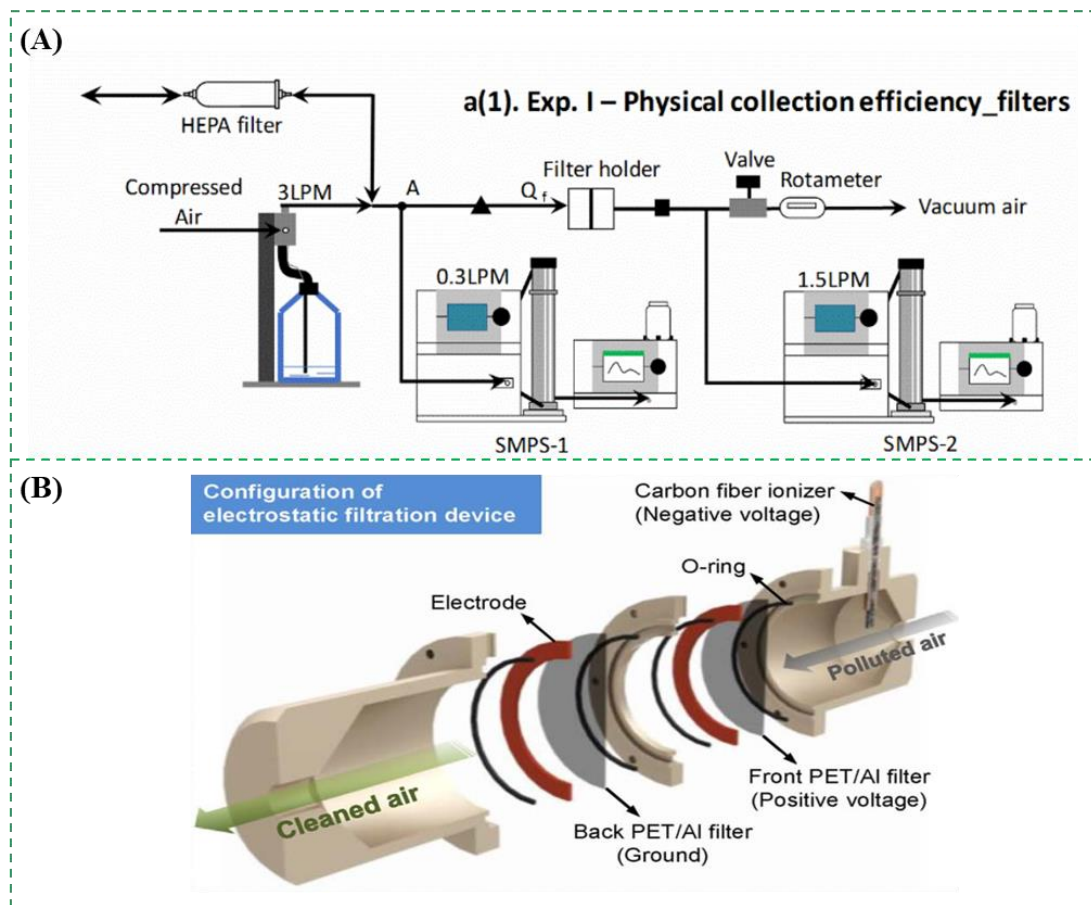


Figure 2. (A) The filtration method for collection of bioaerosols containing influenza virus. Reprinted with permission from ref. [39]. Copyright 2018 Elsevier B.V. (B) The filtration method for collection of bioaerosols containing *Escherichia coli* and *Staphylococcus epidermidis*. Reprinted with permission from ref. [40]. Copyright 2018 Elsevier B.V.

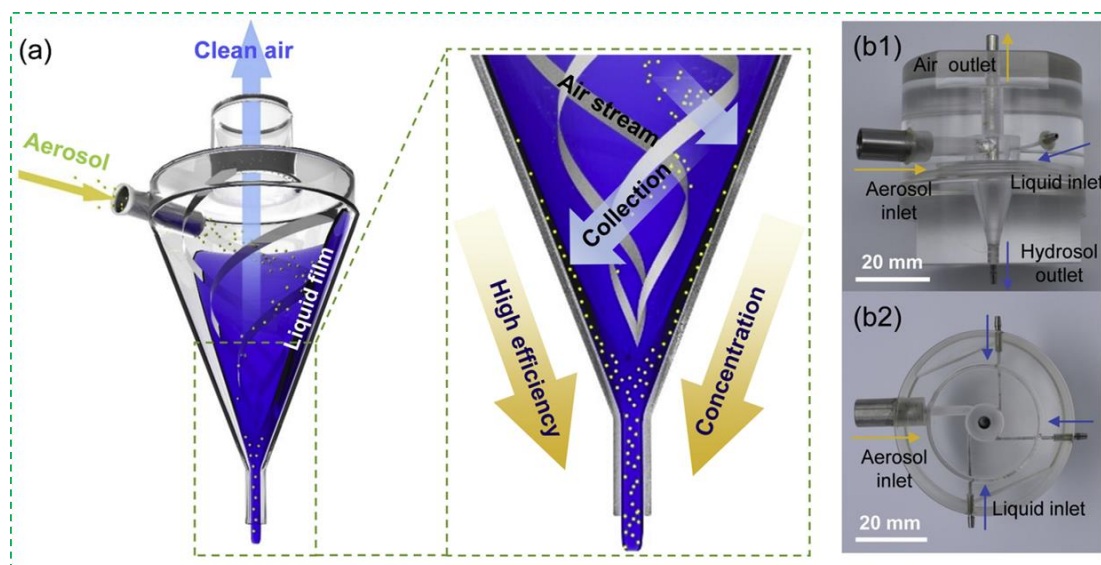


Figure 3. The centrifugation method for collection of the bioaerosols containing *Staphylococcus epidermidis*, *Micrococcus luteus*, and *E. coli*. (a) Schematic diagram of the operating principle of the wet-cyclone; (b1) Front- and (b2) top-view photographs of the wet-cyclone module. Reprinted with permission from ref. [46]. Copyright 2019 Elsevier B.V.

The centrifugation method has shown its merits of compact size, high efficiency, and continuous-flow collection. However, it still has some limitations, such as (1) the low collection efficiency for smaller bioaerosols ($<1 \mu\text{m}$), (2) the evaporation of the thin liquid film, and (3) the difficult control of the gas and liquid flows.

2.4. Impaction

The impaction method is based on inertia to collect the bioaerosols. Generally, the bioaerosols are first drawn into a nozzle using a vacuum pump. Then, the bioaerosols are impacted onto a solid collection medium (such as glass slide, agar plate, filter, gelatin, etc.), which is perpendicular to the nozzle's outlet. Finally, the bioaerosols with higher inertia are captured onto the medium, while those with lower inertia flee with the air flow [43,48,49]. Usually, a single-stage impactor, which only needs a set of nozzles and a collection medium, has its cut-off size. The bioaerosols larger than the cut-off size can be effectively collected in the collection medium. While a multi-stage impactor is often used to study the size distribution of bioaerosols due to the gradually smaller nozzles and continuous-flow collection media. There are some commercially available impactors, such as Anderson impactors (WesTech, Salt Lake City, UT, USA), Aerotech impactors (Aerotech Laboratories, Coventry, UK), BioImpactor (AES, Combourg, France), and BioStage impactors (SKC Inc., Covington, GA, USA), etc. [2]. A typical example was shown in Figure 4A. The bioaerosols containing *Escherichia coli* cells were continuous-flow collected by the impactor onto an agarose gel with fluorescent dye and directly detected using a mini-fluorescence microscope to take in situ fluorescent images. The results showed that the collection efficiency of this impactor for the bioaerosols above a diameter of $0.84 \mu\text{m}$ was over 50% at the flow rate of 10 L/min [50]. Another example was reported by Ozcan et al. and shown in Figure 4B. An impaction method was combined with a digital holographic microscope for label-free detection and automatic classification of the bioaerosols. The bioaerosols were first collected in the substrate using the impaction method. Then, the microscope was used to record the diffraction holograms with the amplitude and phase data of each individual bioaerosol, which were further analyzed using an image processing software to classify the bioaerosols into pre-trained classes based on the deep convolutional neural networks. The results showed that this method could achieve $> 94\%$ classification accuracy for the bioaerosols [51].

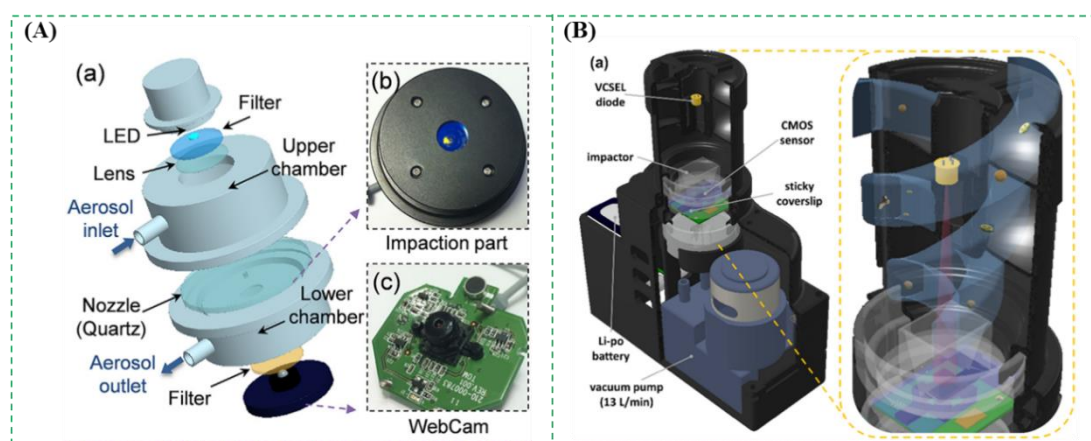


Figure 4. (A) The impactor for collection of the bioaerosols containing *Escherichia coli*. Reprinted with permission from ref. [50]. Copyright 2017 Elsevier B.V. (B) The impactor combined with holographic microscopy and deep-learning for detection of the bioaerosols. Reprinted with permission from ref. [51]. Copyright 2018 American Chemical Society.

At present, the impaction method has been widely applied to collect the bioaerosols because it is cost-effective, easy-to-use, and without additional post-processing. However, it also has some limitations, including (1) reduced collection efficiency due to the deposition

of bioaerosols on the wall of impactors and the possible bounce of bioaerosols; (2) decreased bioactivity because of the shear force on the bioaerosols, the impaction on the collection medium and the desiccation of the bioaerosols; and (3) the difficulty of enumeration of the colonies in the collection medium due to the overlap of microorganisms.

2.5. Impingement

The impingement method is similar to the impaction one, and the difference is the use of a liquid collection medium. Usually, the bioaerosols are sucked into a chamber through nozzles and captured by the liquid collection medium when they strike the medium [52–55]. There are some commercial impingers, such as All-Glass Impinger (Ace Glass Inc., Vineland, USA), SKC BioSampler (SKC Inc., Covington, GA, USA), Multistage Liquid Impinger (Burkard Manufacturing Co. Ltd., Rickmansworth, UK), etc. A typical impinger was shown in Figure 5A. It was able to collect 25% of the bioaerosols with the size of <500 nm and 69–99% of those with larger sizes at the flow rate of 3.1×10^3 L/min [56]. As shown in Figure 5B, the collection efficiencies of SKC BioSampler for aerosolized bacterial species from 0.5 to 10 μm were studied using an Ultraviolet Aerodynamic Particle Sizer unit. The results showed that the overall collection efficiencies of all viable biological particles were 95.3%, 87.7%, and 65.5%, respectively, for different volumes of collection liquids 20 mL, 10 mL, and 5 mL at the flow rate of 12.5 L/min [57].

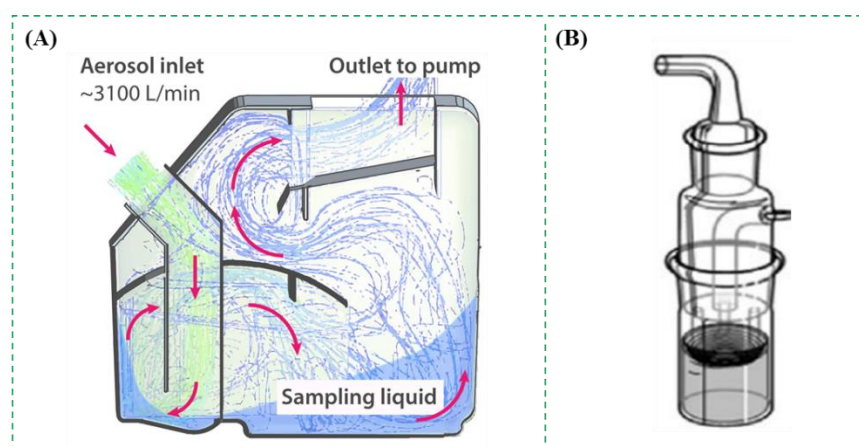


Figure 5. (A) The impinger for collection of the bioaerosols. Reprinted with permission from ref. [56]. Copyright 2017 American Chemical Society. (B) The liquid impinger BioSampler for collection of bioaerosol particles [57]. Reprinted with permission from ref. [57]. Copyright 2017 Elsevier B.V.

These impingers can collect the bioaerosols containing pathogenic microorganisms in the liquid buffer solution, which can be directly detected without an additional elution process. Although the impingement methods have been used as a reference in many studies [58], there are some limitations for their practical applications, including: (1) reduced viability due to the shear forces in the nozzles and the turbulence caused by the air; (2) the evaporation of the liquid collection medium; and (3) the adherence of partially collected particles onto the wall of the collection chamber.

2.6. Microfluidics

Microfluidic chips featured with miniaturization, integration, and multifunction have been widely used in environmental monitoring [59,60], food safety [61–63], medical diagnosis [64–66], etc. Recently, microfluidic chips are increasingly exploited for bioaerosol collection, which either relied on different structures of the microfluidic chips, such as the staggered herringbone for generation of the chaotic vortex [67], the curved, circle or spiral channels for production of the centrifugal forces [68], or combined with the traditional bioaerosol collection methods to develop simpler, inexpensive, and portable methods [69].

As shown in Figure 6A, a microfluidic chip with the staggered herringbone structures was designed to enrich the bioaerosols containing *Mycobacterium tuberculosis*. Due to the staggered herringbone structures, the chaotic flow was induced to create more chances for the collision between the bacteria and the inside wall of channels, resulting in the high capture efficiency (almost 100%) within 20 min [70]. As shown in Figure 6B, another microfluidic chip with the curved microchannel was used to collect bioaerosols into liquids. Due to the centrifugal and drag forces on the bioaerosols, the direction of bioaerosols was changed towards the liquid. The results showed that the collection efficiency was $\sim 90\%$ for the bioaerosols containing *S. epidermidis* with a specific geometric mean diameter of $\sim 0.79 \mu\text{m}$ [71]. Besides, in Figure 6C, a simple microfluidic chip combined with a microfilter achieved a high collection efficiency of 99% for bioaerosols with a diameter $< 1 \mu\text{m}$ [72]. The microfluidic chips have shown their merits, such as low cost, easy integration, and automatic operation, but their low flow rate and short collection duration lead to the small sampling volume.

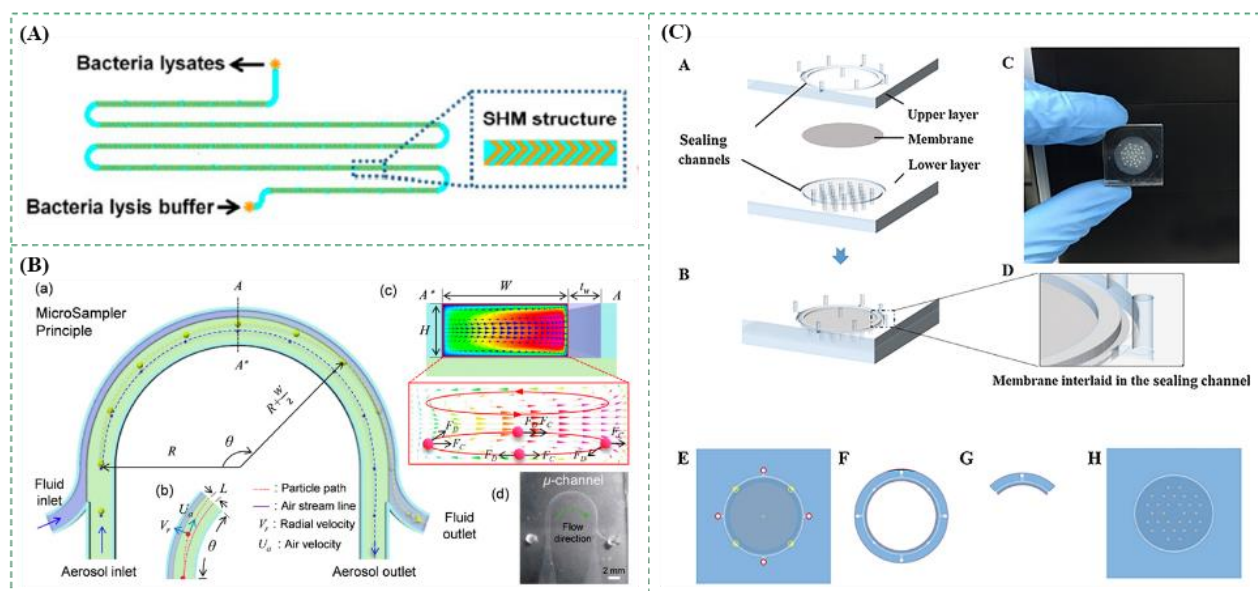


Figure 6. (A) The microfluidic chip with staggered herringbone structures for collection of the bioaerosols containing *Mycobacterium tuberculosis*. Reprinted with permission from ref. [70]. Copyright 2014 American Chemical Society. (B) The microfluidic chip with curved microchannel for collection of the bacterial bioaerosols. Reprinted with permission from ref. [71]. Copyright 2017 American Chemical Society. (C) The microfluidic chip combined with filtration for collection of bioaerosols. Reprinted with permission from ref. [72]. Copyright 2018 Elsevier B.V.

3. Pathogen Detection

The detection of pathogens is an effective method to quantify bioaerosols in the air, which is also another important part of bioaerosol monitoring. The principle, advantages, and disadvantages of pathogen detection methods are summarized in this section. Some examples with different bioaerosol detection methods were compared in Table 1. All of these methods are able to detect pathogens, but the molecular biological and immunological detection methods are obviously faster than the culture method.

3.1. Microbial Culture

The microbial culture is the most common method for detection of the pathogens in the bioaerosols [73–78]. Take pathogenic bacteria in the bioaerosols as an example. After the bioaerosols are collected, they are first suspended in the buffer solution and then surface plated on the agar plates, followed by incubation at the appropriate temperature for sufficient time to form the visible colonies, which are finally counted to determine the

concentration of the bioaerosols. Since there are often some non-target microorganisms in the air, the non-selective culture medium can be used to cultivate all the microorganisms in the bioaerosols, while the selective culture medium can be used to cultivate only the specific microorganisms. An interesting study was reported by Schäfer et al. using the agar plates to cultivate the bioaerosols containing bacteria at the proper temperature for several days, which was further combined with subsequent colony counting procedures to analyze the diversity of the target bacteria in the bioaerosols [79,80]. The microbial culture is simple, accurate and effective; however, it has some limitations, including that it is: (1) time-consuming (over 24 h); (2) not applicable for the non-cultural pathogens; (3) not suitable for in-field applications.

3.2. Molecular Biological Detection

Molecular biological detection methods have made considerable progress over the past decades [81,82]. PCR is the representative method for molecular biological detection, which is able to quantitatively and specifically detect various pathogens in the bioaerosols [83–89]. After the bioaerosols were collected and lysed to release the nucleic acids from target microorganisms, the nucleic acids were denatured, annealed, and extended to achieve their amplification. Hernández et al. used real-time PCR to rapidly detect *Enterococcus faecalis*, which were collected in a filter, with high sensitivity and good specificity [90]. For those bioaerosols containing RNA viruses, after RNA was extracted and reversely transcribed into DNA, the same procedure could be performed as DNA. The SARS-CoV-2 is a kind of RNA virus and could be detected using reverse transcription PCR (RT-PCR) [91]. Aoki et al. combined an IgG assay with RT-PCR to detect the SARS-CoV-2. The results showed that this combination of RT-PCR and IgG assay could improve the robustness for laboratory diagnosis of COVID-19 [92]. Recently, microfluidic chips, which are able to integrate mixing, washing, incubation, reaction and detection onto a single chip, are often used with molecular biological assays for detection of pathogens in the bioaerosols [93]. As shown in Figure 7, a microfluidic device was combined with a photothermal system to capture, lyse, and detect the bacteria in the bioaerosols. The bioaerosols were first captured by the microfluidic herringbone chip and then irradiated with a 532 nm laser, resulting in a photothermal effect of spherical gold nanoparticles in the chip and thus the thermal lysis of bacteria. Finally, the extracted biomacromolecules were analyzed for quantitative detection of bioaerosols [94]. A thermoplasmonic-assisted dual-mode transducer was presented to detect the SARS-CoV-2 viruses in 30 min, where an amplification-free-based direct viral RNA detection and an amplification-based cyclic fluorescence probe cleavage detection were combined and demonstrated as a potential tool for fast clinical infection screening and real-time environmental monitoring [95]. Besides, some other molecular biological detection methods were also applied to detect the SARS-CoV-2 viruses [96,97]. Liu et al. developed a 3D printed microfluidic chip to detect the SARS-CoV-2 viruses using a Flinders membrane for nucleic acid extraction, recombinase polymerase amplification, and loop-mediated isothermal amplification for sensitive detection, a smartphone-based platform for colorimetric signal monitoring. The result showed that this microfluidic chip was able to detect SARS-CoV-2 as low as 100 GE/mL [98].

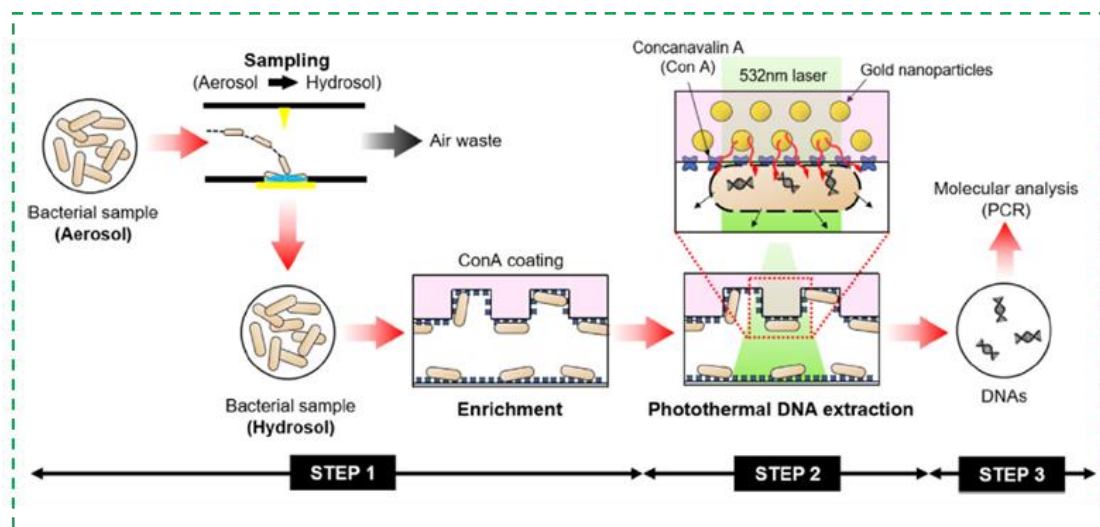


Figure 7. The microfluidic chip for PCR detection of the bacterial bioaerosols. Reprinted with permission from ref. [94]. Copyright 2017 Elsevier B.V.

In theory, conventional PCR is not able to discriminate viable and non-viable microorganisms, resulting in possible overestimation of pathogenic microorganisms in the bioaerosols. In recent years, some specific intercalating photo-reactive reagents were reported to pretreat the bacterial cells to form covalent bonds with the DNA of dead cells, so that only the DNA of live cells could be amplified and detected using PCR. Propidium monoazide (PMA) and ethidium monoazide (EMA) are two effective intercalating reagents, which only permeate cells with disrupted cell membrane, rendering the DNA unavailable for amplification [99–101]. Chen et al. developed a PMA-quantitative PCR method, which was able to quantify the viable bacteria in the bioaerosols with the linear range of 10^4 to 10^{10} CFU/mL [102]. However, the PMA and EMA at higher concentrations are toxic, thus limiting their practical applications.

Compared to the microbial culture, the molecular biological detection methods are of rapid detection, high sensitivity, and good specificity, and have been widely applied for detection of pathogens in the bioaerosols. However, they also have some limitations, including (1) high skill due to complex nucleic acid extraction; (2) potential cross-contamination due to the leakage of nucleic acid templates; (3) laboratory dependence due to benchtop instrument.

3.3. Immunological Detection

The immunological detection methods are based on the antibody-antigen reaction. In the past decades, various biosensors for detection of the pathogens in the bioaerosols have received increasing attention due to their outstanding features of low cost, fast response, miniature size, and easy integration, and have been considered as a promising candidate for in-field applications in many fields, such as biomedical diagnostics, food safety, environmental monitoring, and so on [45,103,104].

Electrochemical biosensors are one of the most common biosensors, which convert biological signals into electrical ones, including impedance, current, potential, etc., resulting from enzymatic catalysis, redox reaction, and antigen-antibody binding, etc. An interesting study on electrochemical biosensors was shown in Figure 8A using single-walled carbon nanotubes (SWCNTs) to detect *Bacillus subtilis* in the bioaerosols. The bioaerosols containing *Bacillus subtilis* were captured by the polyclonal antibodies immobilized on the SWCNTs-based biosensor, resulting in the change in the electric resistance, which was measured using a potentiostat. This electrochemical biosensor was able to detect *Bacillus subtilis* from 10^2 to 10^{10} CFU/mL within 10 min with the detection limit of 10^2 CFU/mL [105].

The field effect transistor (FET) biosensors are based on the measurement of drain current and have been reported to detect the pathogens in the bioaerosols [30]. The metal gates in metal-oxide-semiconductor FET structures were often replaced by ion-sensitive membranes (ISMs) and reference electrodes modified by biological elements (such as antibodies and antigens). When the charged biological targets were recognized to form the complexes on the ISMs, or the biological targets on the ISMs induced biochemical reactions to produce ionic products (such as H^+). As a result, the density of surface charges on the ISM was changed, resulting in the change in the ISM potential and thus the change in drain current. Therefore, the drain current was measured to quantitatively determine the number of targets. As shown in Figure 8B, Lee et al. reported a two-channel carbon nanotube FET (CNT-FET) to simultaneously detect the bioaerosols containing two different fungi collected by the impinger. When the negatively charged fungi were conjugated with the antibodies immobilized on the CNT-FET, a negative gating effect was applied to the CNT channel, resulting in an increase in the current. This CNT-FET biosensor was able to simultaneously detect *Alternaria alternata* and *Aspergillus niger* from 10^1 to 10^6 pg/mL [106]. Besides, as shown in Figure 8C, a real-time monitoring system for the bioaerosols containing influenza H3N2 viruses was designed by integrating a FET sensor, a microfluidic chip, and a bioaerosol-to-hydrosol air sampler. When the bioaerosols containing H3N2 viruses were collected into the buffer solution by the air sampler and injected into the microfluidic chip, the viruses were captured by the antibody-modified FET sensor, resulting in the discrete conductance changes. The results showed that when the concentration of viruses increased 10 times, the FET sensor response increased about 20–30% [107].

Piezoelectric biosensors are based on the change of the mass and have been used in the fields of analytical chemistry, environmental monitoring, and gas detection. Quartz crystal microbalance (QCM) biosensors and surface acoustic wave (SAW) biosensors are two main kinds of piezoelectric biosensors. The QCM biosensor measures the change in the frequency of quartz crystal resonator resulting from the mass change. Generally, the antibodies are modified onto the gold surface of the quartz crystal resonator to specifically capture the targets in the bioaerosols, resulting in the increase in the mass on the surface and thus the decrease in the resonance frequency [108,109]. Skladal et al. proposed a QCM biosensor, which was able to detect the bioaerosols containing *Escherichia coli* with a lower detection limit of 1.45×10^4 CFU/L in 16 min [110]. The SAW biosensor mainly consists of a piezoelectric material, an interdigital transducer, and an oscillation circuit, and measures the change in the viscoelasticity, mass, or frequency of a liquid [111–114]. As shown in Figure 8D, Mitsubayashi et al. developed an enhanced SAW biosensor for sensitive detection of the bioaerosols containing the house dust mite (HDM) allergens. First, the surface of the SAW transducer was modified with a self-assembled monolayer of the mixture of ORLA85, 6PEG-thiol and capture antibodies. Then, the HDM allergens, *Dermatophagoides farinae*, were dropped and incubated for 10 min. After washing with PBS, the HRP modified detection antibodies were dropped and incubated for 10 min to label the targets. Finally, the substrate was added and catalyzed by HRP for 2 min to produce the precipitates on the surface of SAW biosensor, resulting in the change in the velocity of the surface acoustic wave and thus a phase shift. The results showed that the precipitates greatly increased the mass on the surface of the SAW biosensor, and this SAW biosensor had a detection limit as low as 35 pg/mL [115].

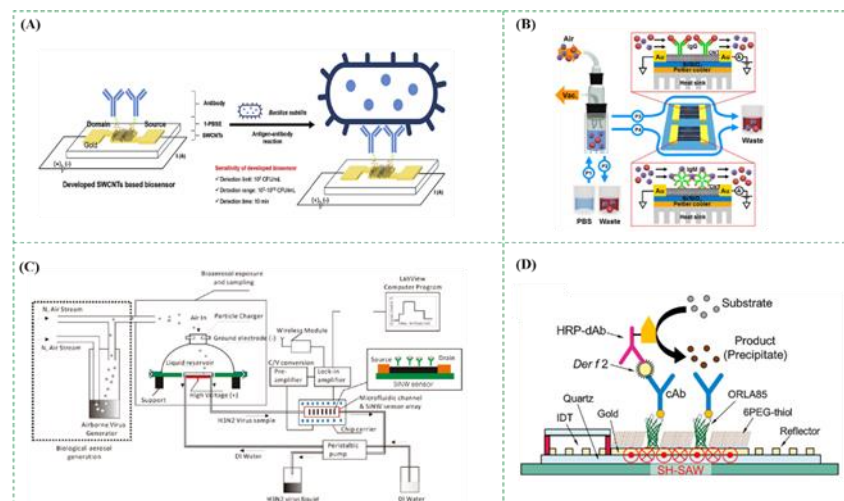


Figure 8. (A) The electrochemical biosensor for detection of the bioaerosols containing *Bacillus subtilis*. Reprinted with permission from ref. [105]. Copyright 2017 Elsevier B.V. (B) The FET biosensor for detection of the bioaerosols containing *Alternaria alternata* and *Aspergillus niger*. Reprinted with permission from ref. [106]. Copyright 2016 American Chemical Society. (C) The FET biosensor on microfluidic chips for detection of the bioaerosols containing influenza H3N2 viruses. Reprinted with permission from ref. [107]. Copyright 2011 American Chemical Society. (D) The SAW biosensor for detection of the bioaerosols containing house dust mite allergens. Reprinted with permission from ref. [115]. Copyright 2019 Elsevier B.V.

Surface plasmon resonance (SPR) biosensors rely on the change of refractive index resulted from the mass accumulation at the sensing surface to quantify the targets from small molecules to the whole microbes, such as proteins, viruses, bacteria, and so on [116]. Similarly, the biological components were immobilized on the surface of the SPR sensor, followed by reaction with the targets, leading to the change of the mass on the surface [117]. Agranovski et al. reported an SPR biosensor for rapid detection of the bioaerosols containing bacteria. The SPR sensor was first modified with the biotinylated rabbit polyclonal anti-*E. coli* antibodies. Then, the *E. coli* cells were specifically captured by the antibodies onto the surface. The change of the refractive index was finally measured to determine the concentration of the target bacteria. This SPR biosensor could detect the bioaerosols containing *E. coli* from 1.5×10^3 to 1.5×10^8 CFU/mL [118]. Wang et al. developed a succinimidyl-ester-functionalized plasmonic biosensor for accurate and fast detection of total bioaerosols in different environments, which could be a reliable candidate for air quality assessment. The detection limits of this biosensor for bioaerosols containing *Escherichia coli* and *Bacillus subtilis* were 0.5119 and 1.69 cells/mL, respectively [119].

3.4. Others

There are also some other methods for detection of the pathogens in bioaerosols, such as flow cytometry [120], laser induced fluorescence [121,122], laser induced breakdown spectroscopy [123], epifluorescence microscopy [124,125], matrix-assisted laser desorption/ionization time of flight (MALDI-TOF) [126], Raman spectroscopy [127], transmission electron microscopy [128], scanning electron microscope [129], ATP-based bioluminescence assay [130], etc.

Adenosine triphosphate (ATP), as an energy substance, is commonly found in live cells [131]. The ATP-based bioluminescence assay is based on the measurement of the light resulted from the reaction between luciferin and luciferase. Based on the known relationship between the light intensity and the ATP concentration, the concentration of target microorganisms in the bioaerosols could be obtained. As an available and affordable method, the ATP-based bioluminescence assay has been extensively applied for rapid detection of the pathogens in the bioaerosols [55,132,133]. As shown in Figure 9A, Jung

et al. used the ATP-based bioluminescence assay for real-time detection of the bioaerosols. The luciferase-luciferin mixtures were first dropped and immobilized on the glass-fiber pad. After the bioaerosols were collected using wet cyclone and lysed using thermal lysis, the lysed sample was dropped to the pad every 2 min. The bioluminescent intensity of the pad was finally measured using the photomultiplier tube. This bioluminescence assay was able to detect the bioaerosols with pathogenic microorganisms as low as ~ 130 CFU/m³ in seconds [47]. Besides, as shown in Figure 9B, the bioaerosols containing bacteria were first charged by the negative ions and then collected in a flowing liquid containing cell lysis buffer and ATP bioluminescence reagents. After the liquid was delivered to the microfluidic chip, the collected bacteria were dissolved by the cell lysis buffer, and ATP was extracted and detected by the bioluminescence detector. The total detection time was 30 s at a liquid flow rate of 800 μ L/min [34].

Table 1. Comparison of bioaerosol detection methods.

| Detection Method | Target | Detection Range | Detection Time | LOD | References |
|---------------------------------|---------------------------------|---|----------------|--|------------|
| Culture | <i>Enterococcus</i> | - | 24 h | 10 ³ CFU/mL | [76] |
| PCR | <i>Enterococcus faecalis</i> | 1.5 × 10 ³ –1.5 × 10 ⁸ CFU/mL | 72 min | 1.5 × 10 ³ CFU/mL | [90] |
| RT-PCR | Bovine viral diarrhea virus | 5.2 × 10 ⁰ –5.2 × 10 ⁸ RNA molecules | <30 min | 5.2 RNA molecules | [134] |
| RT-PCR | Influenza virus | 3.7 × 10 ⁴ –3.7 × 10 ⁶ TCID ₅₀ /mL | <50 min | 3.7 × 10 ⁴ TCID ₅₀ /mL | [135] |
| Chemiluminescence immunoassays | <i>Legionella</i> | 8 × 10 ³ –8 × 10 ⁶ cells/mL | 1 h | 1 × 10 ³ cells/mL | [104] |
| Chemiluminescence immunoassays | <i>Dermatophagoides farinae</i> | 0.49–250 ng/mL | - | 0.49 ng/mL | [136] |
| Electrochemical biosensor | <i>Escherichia coli</i> DH5a | 10 ³ –10 ⁸ CFU/mL | 20 min | 150 CFU/mL | [137] |
| Electrochemical biosensor | <i>Bacillus subtilis</i> | 10 ² –10 ¹⁰ CFU/mL | 10 min | 10 ² CFU/mL | [105] |
| FET biosensor | <i>Alternaria alternate</i> | 10 ¹ –10 ⁶ pg/mL | - | 10 pg/mL | [106] |
| QCM biosensor | Cat allergens | 5.2 × 10 ⁰ –1.6 × 10 ⁵ ng/L | 30 min | 5.2 ng/L | [108] |
| QCM biosensor | <i>Escherichia coli</i> | 1.45 × 10 ⁴ –1.45 × 10 ⁶ CFU/L | 16 min | 10 ⁴ CFU/L | [109] |
| SAW biosensor | Dust mite allergens | 10 ⁰ –10 ³ ng/mL | 24 min | 6.1 ng/mL | [111] |
| SAW biosensor | Dust mite allergens | 1.0–3000 ng/mL | 20 min | 6.3 ng/mL | [112] |
| SAW biosensor | Dust mite allergens | 0.3–1000 ng/mL | 36 min | 2.5 ng/mL | [113] |
| SAW biosensor | Dust mite allergens | 10 ² –3 × 10 ³ ng/mL | - | 20.1 ng/mL | [114] |
| SAW biosensor | Dust mite allergens | 0.08–1 ng/mL | - | 35 pg/mL | [115] |
| SPR biosensor | MS2 phage | 2.2 × 10 ⁶ –2.2 × 10 ¹¹ PFU/mL | <1 min | 1.12 × 10 ⁶ PFU/mL | [116] |
| SPR biosensor | <i>Escherichia coli</i> | 1.5 × 10 ³ –1.5 × 10 ⁸ CFU/mL | - | 1.5 × 10 ³ CFU/mL | [118] |
| ATP-based bioluminescence assay | <i>Escherichia coli</i> | 10 ³ –10 ⁸ CFU/mL | 5 min | 2.32 × 10 ³ CFU/mL | [55] |
| ATP-based bioluminescence assay | <i>Escherichia coli</i> | 3.7 × 10 ¹ –3.7 × 10 ⁷ CFU/mL | 5 min | 375 CFU/mL | [47] |

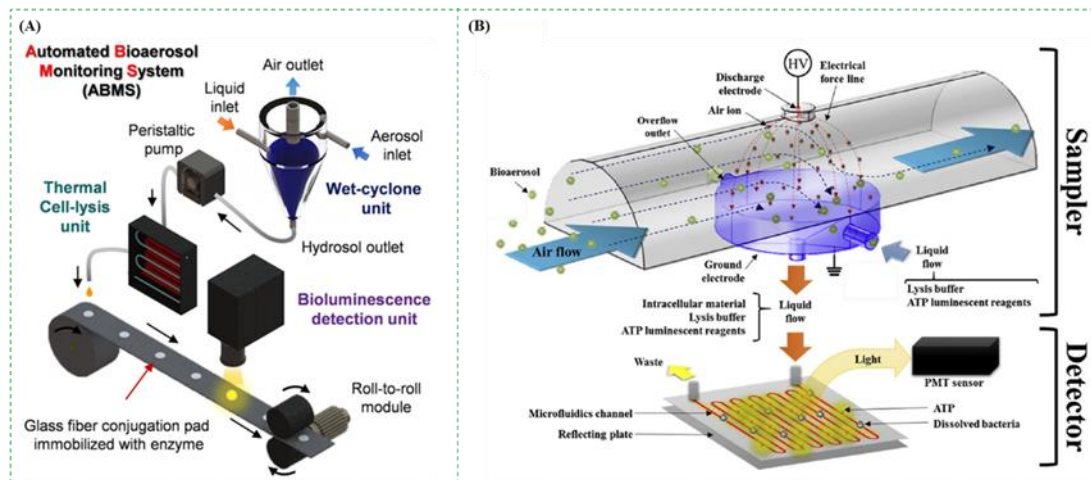


Figure 9. (A) The ATP-based bioluminescence assay for real-time detection of the bioaerosols. Reprinted with permission from ref. [47]. Copyright 2020 American Chemical Society. (B) The ATP-based bioluminescence assay on microfluidic chip for detection of the bacterial bioaerosols. Reprinted with permission from ref. [34]. Copyright 2016 Elsevier B.V.

This assay also showed its ability to distinguish the presence of viable but non-cultivable microorganisms. However, this assay still suffered from some limitations, including (1) significant reduction in the activity of luciferase due to prolonged exposure to the liquid phase; (2) decreased detection accuracy and stability due to the presence of other chemicals; (3) low selectivity for detection of the bioaerosols containing spores due to the low level of ATP in spores.

4. Conclusions and Future Trends

The monitoring of bioaerosols containing pathogenic microorganisms is very important for prevention and control of airborne diseases. The collection and detection of bioaerosols are the essential procedures for bioaerosol monitoring. The existing bioaerosol collection and detection methods basically have an impact on the bioactivity of bioaerosols, which should be further investigated to better understand the risk level of the bioaerosols and even to develop the inactivation methods for bioaerosols.

For the collection of bioaerosols, the electrostatic sedimentation, the centrifugation, the impaction, and the impingement methods might damage the bioactivity of collected bioaerosols to a certain extent, which might result in the underestimation of the risk level of bioaerosols. These methods have higher collection efficiency for collecting the bioaerosols with micrometer-scale microorganisms due to their more charges or bigger mass. Besides, these methods using liquid collection medium often have higher recovery than those using solid medium because extra washing procedure is not required. Some samplers like PTFE filters, gelatin filters, and cyclones were able to collect the SARS-CoV-2 viruses which were followed by RT-PCR analysis [138]. Besides, the microfluidic chips have shown their obvious advantages over the traditional methods and they are indeed promising to develop online collection methods. However, the concentration of pathogen microorganisms in the air is usually very low, and thus the collected bioaerosols are often few and cannot be directly detected using the existing detection methods due to their limited sensitivity. Therefore, a large volume of air samples might be used to collect enough bioaerosols for downstream detection, and more efficient collection methods should be further investigated and developed.

For the detection of bioaerosols, the microbial culture has high sensitivity and accuracy but needs a long time to get final results. PCR is fast and sensitive but needs complex DNA extraction procedures. Various biosensors with low cost, fast response, miniature size, and easy integration, have received increasing attention and been considered as effective tools for detection of bioaerosols. At present, bioaerosol monitoring generally

includes two separate procedures: bioaerosol collection and pathogen detection and cannot be achieved in real-time. The integration of bioaerosol collection and detection onto a single chip is still a big challenge, but it is urgently demanded for online monitoring of bioaerosols containing pathogenic microorganisms. Besides, dead and live microorganisms always coexist in the bioaerosols, and most detection methods still cannot distinguish between dead and live microorganisms, leading to overestimation of the pathogens in the bioaerosols. Thus, it is vital to develop detection methods that are able to distinguish dead and live microorganisms.

With rapid development of the Internet of Things (IOT), bioaerosol monitoring should be tightly integrated with the IOT to achieve a more efficient response to the potential risks. The detection results for bioaerosol monitoring can be combined with the collection data (including environmental temperature, environmental humidity, sampling time, sampling location, sampling person, sample ID, etc.) and detection data (including testing person, testing time, testing method, etc.), and transmitted to bioaerosol monitoring cloud platforms through wireless communication. The detection results can be dynamically analyzed using artificial intelligence and big data technologies to predict the risk level of bioaerosols and suggest the response to this risk.

Author Contributions: Conceptualization, M.L. and L.W.; investigation, W.Q. and Y.L.; resources, W.Q. and Y.L.; writing—original draft preparation, M.L. and L.W.; writing—review and editing, J.L.; supervision, J.L.; funding acquisition, J.L. All authors have read and agreed to the published version of the manuscript.

Funding: This work was supported by the China Scholarship Council (201906350176) and the Walmart Foundation (UA2020-154).

Institutional Review Board Statement: Not applicable.

Data Availability Statement: Not applicable.

Conflicts of Interest: The authors declare no conflict of interest.

References

- Kabir, E.; Azzouz, A.; Raza, N.; Bhardwaj, S.K.; Kim, K.-H.; Tabatabaei, M.; Kukkar, D. Recent Advances in Monitoring, Sampling, and Sensing Techniques for Bioaerosols in the Atmosphere. *ACS Sens.* **2020**, *5*, 1254–1267. [[CrossRef](#)] [[PubMed](#)]
- Haig, C.; Mackay, W.; Walker, J.; Williams, C. Bioaerosol sampling: Sampling mechanisms, bioefficiency and field studies. *J. Hosp. Infect.* **2016**, *93*, 242–255. [[CrossRef](#)]
- Pan, M.; Lednicky, J.; Wu, C. Collection, particle sizing and detection of airborne viruses. *J. Appl. Microbiol.* **2019**, *127*, 1596–1611. [[CrossRef](#)]
- Ghosh, B.; Lal, H.; Srivastava, A. Review of bioaerosols in indoor environment with special reference to sampling, analysis and control mechanisms. *Environ. Int.* **2015**, *85*, 254–272. [[CrossRef](#)]
- Xie, W.; Li, Y.; Bai, W.; Hou, J.; Ma, T.; Zeng, X.; Zhang, L.; An, T. The source and transport of bioaerosols in the air: A review. *Front. Environ. Sci. Eng.* **2021**, *15*, 1–19. [[CrossRef](#)]
- World Health Organization. Available online: <https://www.who.int/news-room/fact-sheets/detail/the-top-10-causes-of-death> (accessed on 9 December 2020).
- Tong, T.R. Airborne Severe Acute Respiratory Syndrome Coronavirus and Its Implications. *J. Infect. Dis.* **2005**, *191*, 1401–1402. [[CrossRef](#)]
- Booth, T.F.; Kournikakis, B.; Bastien, N.; Ho, J.; Kobasa, D.; Stadnyk, L.; Li, Y.; Spence, M.; Paton, S.; Henry, B.; et al. Detection of Airborne Severe Acute Respiratory Syndrome (SARS) Coronavirus and Environmental Contamination in SARS Outbreak Units. *J. Infect. Dis.* **2005**, *191*, 1472–1477. [[CrossRef](#)]
- Kim, H.R.; An, S.; Hwang, J. High air flow-rate electrostatic sampler for the rapid monitoring of airborne coronavirus and influenza viruses. *J. Hazard. Mater.* **2021**, *412*, 125219. [[CrossRef](#)] [[PubMed](#)]
- Piri, A.; Kim, H.R.; Park, D.H.; Hwang, J. Increased survivability of coronavirus and H1N1 influenza virus under electrostatic aerosol-to-hydrosol sampling. *J. Hazard. Mater.* **2021**, *413*, 125417. [[CrossRef](#)]
- Da Silva, P.G.; Nascimento, M.S.J.; Soares, R.R.G.; Sousa, S.I.V.; Mesquita, J.R. Airborne spread of infectious SARS-CoV-2: Moving forward using lessons from SARS-CoV and MERS-CoV. *Sci. Total Environ.* **2021**, *764*, 142802. [[CrossRef](#)] [[PubMed](#)]
- Yu, H.C.; Mui, K.; Wong, L.; Chu, H. Ventilation of general hospital wards for mitigating infection risks of three kinds of viruses including Middle East respiratory syndrome coronavirus. *Indoor Built Environ.* **2016**, *26*, 514–527. [[CrossRef](#)]

13. Kim, S.-H.; Chang, S.Y.; Sung-Han, K.; Park, J.H.; BIN Kim, H.; Lee, H.; Choi, J.-P.; Choi, W.S.; Min, J.-Y. Extensive Viable Middle East Respiratory Syndrome (MERS) Coronavirus Contamination in Air and Surrounding Environment in MERS Isolation Wards. *Clin. Infect. Dis.* **2016**, *63*, 363–369. [[CrossRef](#)]
14. Lane, M.A.; Brownsword, E.A.; Morgan, J.S.; Babiker, A.; Vanairsdale, S.A.; Lyon, G.M.; Mehta, A.K.; Ingersoll, J.M.; Lindsley, W.G.; Kraft, C.S. Bioaerosol sampling of a ventilated patient with COVID-19. *Am. J. Infect. Control.* **2020**, *48*, 1540–1542. [[CrossRef](#)]
15. Gholipour, S.; Mohammadi, F.; Nikaeen, M.; Shamsizadeh, Z.; Khazeni, A.; Sahbaei, Z.; Mousavi, S.M.; Ghobadian, M.; Mirhendi, H. COVID-19 infection risk from exposure to aerosols of wastewater treatment plants. *Chemosphere* **2021**, *273*, 129701. [[CrossRef](#)] [[PubMed](#)]
16. Robotto, A.; Quaglino, P.; Lembo, D.; Morello, M.; Brizio, E.; Bardi, L.; Civra, A. SARS-CoV-2 and indoor/outdoor air samples: A methodological approach to have consistent and comparable results. *Environ. Res.* **2021**, *195*, 110847. [[CrossRef](#)] [[PubMed](#)]
17. Mainelis, G. Bioaerosol sampling: Classical approaches, advances, and perspectives. *Aerosol Sci. Technol.* **2019**, *54*, 496–519. [[CrossRef](#)]
18. Franchitti, E.; Pascale, E.; Fea, E.; Anedda, E.; Traversi, D. Methods for Bioaerosol Characterization: Limits and Perspectives for Human Health Risk Assessment in Organic Waste Treatment. *Atmosphere* **2020**, *11*, 452. [[CrossRef](#)]
19. Fung, A.O.; Mykhalova, N. Analysis of Airborne Biomarkers for Point-of-Care Diagnostics. *J. Lab. Autom.* **2013**, *19*, 225–247. [[CrossRef](#)]
20. Mbareche, H.; Brisebois, E.; Veillette, M.; Duchaine, C. Bioaerosol sampling and detection methods based on molecular approaches: No pain no gain. *Sci. Total. Environ.* **2017**, *599–600*, 2095–2104. [[CrossRef](#)]
21. Huffman, J.A.; Perring, A.E.; Savage, N.J.; Clot, B.; Crouzy, B.; Tummon, F.; Shoshanim, O.; Damit, B.; Schneider, J.; Sivaprakasam, V.; et al. Real-time sensing of bioaerosols: Review and current perspectives. *Aerosol Sci. Technol.* **2020**, *54*, 465–495. [[CrossRef](#)]
22. Jing, W.; Zhao, W.; Liu, S.; Li, L.; Tsai, C.-T.; Fan, X.; Wu, W.; Li, J.; Yang, X.; Sui, G. Microfluidic Device for Efficient Airborne Bacteria Capture and Enrichment. *Anal. Chem.* **2013**, *85*, 5255–5262. [[CrossRef](#)] [[PubMed](#)]
23. Han, T.T.; Thomas, N.M.; Mainelis, G. Performance of personal electrostatic bioaerosol sampler (PEBS) when collecting airborne microorganisms. *J. Aerosol Sci.* **2018**, *124*, 54–67. [[CrossRef](#)]
24. Foat, T.; Sellors, W.; Walker, M.; Rachwal, P.; Jones, J.; Despeyroux, D.; Coudron, L.; Munro, I.; McCluskey, D.; Tan, C.; et al. A prototype personal aerosol sampler based on electrostatic precipitation and electrowetting-on-dielectric actuation of droplets. *J. Aerosol Sci.* **2016**, *95*, 43–53. [[CrossRef](#)]
25. Ladhani, L.; Pardon, G.; Meeuws, H.; Van Wesenbeeck, L.; Schmidt, K.; Stuyver, L.; Van Der Wijngaert, W. Sampling and detection of airborne influenza virus towards point-of-care applications. *PLoS ONE* **2017**, *12*, e0174314. [[CrossRef](#)] [[PubMed](#)]
26. Kim, H.R.; Park, J.-W.; Kim, H.S.; Yong, D.; Hwang, J. Comparison of lab-made electrostatic rod-type sampler with single stage viable impactor for identification of indoor airborne bacteria. *J. Aerosol Sci.* **2018**, *115*, 190–197. [[CrossRef](#)]
27. Park, M.; Son, A.; Chua, B. Microorganism-ionizing respirator with reduced breathing resistance suitable for removing airborne bacteria. *Sens. Actuators B Chem.* **2018**, *276*, 437–446. [[CrossRef](#)] [[PubMed](#)]
28. Hyun, J.; Lee, S.-G.; Hwang, J. Application of corona discharge-generated air ions for filtration of aerosolized virus and inactivation of filtered virus. *J. Aerosol Sci.* **2017**, *107*, 31–40. [[CrossRef](#)]
29. La, A.; Zhang, Q.; Levin, D.B.; Coombs, K.M. The Effectiveness of Air Ionization in Reducing Bioaerosols and Airborne PRRS Virus in a Ventilated Space. *Trans. ASABE* **2019**, *62*, 1299–1314. [[CrossRef](#)]
30. Park, K.T.; Cho, D.G.; Park, J.W.; Hong, S.; Hwang, J. Detection of airborne viruses using electro-aerodynamic deposition and a field-effect transistor. *Sci. Rep.* **2015**, *5*, 17462. [[CrossRef](#)] [[PubMed](#)]
31. Roux, J.M.; Sarda-Estève, R.; Delapierre, G.; Nadal, M.H.; Bossuet, C.; Olmedo, L. Development of a new portable air sampler based on electrostatic precipitation. *Environ. Sci. Pollut. Res.* **2016**, *23*, 8175–8183. [[CrossRef](#)] [[PubMed](#)]
32. Afshar-Mohajer, N.; Godfrey, W.H.; Rule, A.M.; Matsui, E.C.; Gordon, J.; Koehler, K. A Low-Cost Device for Bulk Sampling of Airborne Particulate Matter: Evaluation of an Ionic Charging Device. *Aerosol Air Qual. Res.* **2017**, *17*, 1452–1462. [[CrossRef](#)]
33. Hong, S.; Bhardwaj, J.; Han, C.-H.; Jang, J. Gentle Sampling of Submicrometer Airborne Virus Particles using a Personal Electrostatic Particle Concentrator. *Environ. Sci. Technol.* **2016**, *50*, 12365–12372. [[CrossRef](#)]
34. Park, J.-W.; Kim, H.R.; Hwang, J. Continuous and real-time bioaerosol monitoring by combined aerosol-to-hydrosol sampling and ATP bioluminescence assay. *Anal. Chim. Acta* **2016**, *941*, 101–107. [[CrossRef](#)]
35. Priyamvada, H.; Kumaragama, K.; Chrzan, A.; Athukorala, C.; Sur, S.; Dhaniyala, S. Design and evaluation of a new electrostatic precipitation-based portable low-cost sampler for bioaerosol monitoring. *Aerosol Sci. Technol.* **2021**, *55*, 24–36. [[CrossRef](#)]
36. Maestre, J.P.; Jennings, W.; Wylie, D.; Horner, S.D.; Siegel, J.; Kinney, K.A. Filter forensics: Microbiota recovery from residential HVAC filters. *Microbiome* **2018**, *6*, 1–14. [[CrossRef](#)] [[PubMed](#)]
37. Therkorn, J.; Thomas, N.; Scheinbeim, J.; Mainelis, G. Field performance of a novel passive bioaerosol sampler using polarized ferroelectric polymer films. *Aerosol Sci. Technol.* **2017**, *51*, 787–800. [[CrossRef](#)]
38. Hurley, K.V.; Wharton, L.; Wheeler, M.J.; Skjøth, C.A.; Niles, C.; Hanson, M.C. Car cabin filters as sampling devices to study bioaerosols using eDNA and microbiological methods. *Aerobiologia* **2019**, *35*, 215–225. [[CrossRef](#)]
39. Li, J.; Leavey, A.; Wang, Y.; ÓNeil, C.; Wallace, M.A.; Burnham, C.-A.D.; Boon, A.C.; Babcock, H.; Biswas, P. Comparing the performance of 3 bioaerosol samplers for influenza virus. *J. Aerosol Sci.* **2018**, *115*, 133–145. [[CrossRef](#)]

40. Choi, D.Y.; Heo, K.J.; Kang, J.; An, E.J.; Jung, S.-H.; Lee, B.U.; Lee, H.M.; Jung, J.H. Washable antimicrobial polyester/aluminum air filter with a high capture efficiency and low pressure drop. *J. Hazard. Mater.* **2018**, *351*, 29–37. [[CrossRef](#)] [[PubMed](#)]
41. Grayson, S.A.; Griffiths, P.S.; Perez, M.K.; Piedimonte, G. Detection of airborne respiratory syncytial virus in a pediatric acute care clinic. *Pediatr. Pulmonol.* **2017**, *52*, 684–688. [[CrossRef](#)] [[PubMed](#)]
42. Kenny, L.C.; Thorpe, A.; Stacey, P. A collection of experimental data for aerosol monitoring cyclones. *Aerosol Sci. Technol.* **2017**, *51*, 1190–1200. [[CrossRef](#)]
43. Prost, K.; Kloeze, H.; Mukhi, S.; Bozek, K.; Poljak, Z.; Mubareka, S. Bioaerosol and surface sampling for the surveillance of influenza A virus in swine. *Transbound. Emerg. Dis.* **2019**, *66*, 1210–1217. [[CrossRef](#)] [[PubMed](#)]
44. Bekking, C.; Yip, L.; Groulx, N.; Doggett, N.; Finn, M.; Mubareka, S. Evaluation of bioaerosol samplers for the detection and quantification of influenza virus from artificial aerosols and influenza virus-infected ferrets. *Influ. Other Respir. Viruses* **2019**, *13*, 564–573. [[CrossRef](#)] [[PubMed](#)]
45. Sung, G.; Ahn, C.; Kulkarni, A.; Shin, W.G.; Kim, T. Highly efficient in-line wet cyclone air sampler for airborne virus detection. *J. Mech. Sci. Technol.* **2017**, *31*, 4363–4369. [[CrossRef](#)]
46. Cho, Y.S.; Hong, S.C.; Choi, J.; Jung, J.H. Development of an automated wet-cyclone system for rapid, continuous and enriched bioaerosol sampling and its application to real-time detection. *Sens. Actuators B Chem.* **2019**, *284*, 525–533. [[CrossRef](#)]
47. Cho, Y.S.; Kim, H.R.; Ko, H.S.; Bin Jeong, S.; Kim, B.C.; Jung, J.H. Continuous Surveillance of Bioaerosols On-Site Using an Automated Bioaerosol-Monitoring System. *ACS Sens.* **2020**, *5*, 395–403. [[CrossRef](#)] [[PubMed](#)]
48. Chang, C.-W.; Ting, Y.-T.; Horng, Y.-J. Collection efficiency of liquid-based samplers for fungi in indoor air. *Indoor Air* **2019**, *29*, 380–389. [[CrossRef](#)]
49. Alonso, C.; Raynor, P.C.; Davies, P.R.; Torremorell, M. Concentration, Size Distribution, and Infectivity of Airborne Particles Carrying Swine Viruses. *PLoS ONE* **2015**, *10*, e0135675. [[CrossRef](#)] [[PubMed](#)]
50. Choi, J.; Kang, J.S.; Hong, S.C.; Bae, G.-N.; Jung, J.H. A new method for the real-time quantification of airborne biological particles using a coupled inertial aerosol system with in situ fluorescence imaging. *Sens. Actuators B Chem.* **2017**, *244*, 635–641. [[CrossRef](#)]
51. Wu, Y.; Calis, A.; Luo, Y.; Chen, C.; Lutton, M.; Rivenson, Y.; Lin, X.; Koydemir, H.C.; Zhang, Y.; Wang, H.; et al. Label-Free Bioaerosol Sensing Using Mobile Microscopy and Deep Learning. *ACS Photonics* **2018**, *5*, 4617–4627. [[CrossRef](#)]
52. Lindsley, W.G.; Blachere, F.M.; Beezhold, D.; Thewlis, R.E.; Noorbakhsh, B.; Othumpangat, S.; Goldsmith, W.T.; McMillen, C.M.; Andrew, M.E.; Burrell, C.N.; et al. Viable influenza A virus in airborne particles expelled during coughs versus exhalations. *Influ. Other Respir. Viruses* **2016**, *10*, 404–413. [[CrossRef](#)] [[PubMed](#)]
53. Cooper, C.W.; Aithinne, K.; Floyd, E.L.; Stevenson, B.S.; Johnson, D.L. A comparison of air sampling methods for *Clostridium difficile* endospore aerosol. *Aerobiologia* **2019**, *35*, 411–420. [[CrossRef](#)]
54. Ferguson, R.M.W.; Garcia-Alcega, S.; Coulon, F.; Dumbrell, A.J.; Whitby, C.; Colbeck, I. Bioaerosol biomonitoring: Sampling optimization for molecular microbial ecology. *Mol. Ecol. Resour.* **2019**, *19*, 672–690. [[CrossRef](#)]
55. Nguyen, D.T.; Kim, H.R.; Jung, J.H.; Lee, K.-B.; Kim, B.C. The development of paper discs immobilized with luciferase/D-luciferin for the detection of ATP from airborne bacteria. *Sens. Actuators B Chem.* **2018**, *260*, 274–281. [[CrossRef](#)]
56. Šantl-Temkiv, T.; Amato, P.; Gosewinkel, U.; Thyrhaug, R.; Charton, A.; Chicot, B.; Finster, K.; Bratbak, G.; Löndahl, J. High-Flow-Rate Impinger for the Study of Concentration, Viability, Metabolic Activity, and Ice-Nucleation Activity of Airborne Bacteria. *Environ. Sci. Technol.* **2017**, *51*, 11224–11234. [[CrossRef](#)]
57. Zheng, Y.; Yao, M. Liquid impinger BioSampler’s performance for size-resolved viable bioaerosol particles. *J. Aerosol Sci.* **2017**, *106*, 34–42. [[CrossRef](#)]
58. Pardon, G.; Ladhani, L.; Sandström, N.; Ettore, M.; Lobov, G.; van der Wijngaart, W. Aerosol sampling using an electrostatic precipitator integrated with a microfluidic interface. *Sens. Actuators B Chem.* **2015**, *212*, 344–352. [[CrossRef](#)]
59. Huang, Y.; Han, Y.; Gao, Y.; Gao, J.; Ji, H.; He, Q.; Tu, J.; Xu, G.; Zhang, Y.; Han, L. Electrochemical sensor array with nanoporous gold nanolayer and ceria@gold corona-nanocomposites enhancer integrated into microfluidic for simultaneous ultrasensitive lead ion detection. *Electrochim. Acta* **2021**, *373*, 137921. [[CrossRef](#)]
60. Zhang, X.; Chen, X.; Yao, Y.; Shang, X.; Lu, H.; Zhao, W.; Liu, S.; Chen, J.; Sui, G. A disc-chip based high-throughput acute toxicity detection system. *Talanta* **2021**, *224*, 121867. [[CrossRef](#)]
61. Qi, W.; Zheng, L.; Wang, S.; Huang, F.; Liu, Y.; Jiang, H.; Lin, J. A microfluidic biosensor for rapid and automatic detection of Salmonella using metal-organic framework and Raspberry Pi. *Biosens. Bioelectron.* **2021**, *178*, 113020. [[CrossRef](#)] [[PubMed](#)]
62. Chen, P.; Chen, C.; Su, H.; Zhou, M.; Li, S.; Du, W.; Feng, X.; Liu, B.-F. Integrated and finger-actuated microfluidic chip for point-of-care testing of multiple pathogens. *Talanta* **2021**, *224*, 121844. [[CrossRef](#)]
63. Tsougeni, K.; Kaprouac, G.; Loukas, C.; Papadakis, G.; Hamiot, A.; Eck, M.; Rabus, D.; Kokkoris, G.; Chatzandroulis, S.; Papadopoulos, V.; et al. Lab-on-Chip platform and protocol for rapid foodborne pathogen detection comprising on-chip cell capture, lysis, DNA amplification and surface-acoustic-wave detection. *Sens. Actuators B Chem.* **2020**, *320*, 128345. [[CrossRef](#)]
64. Liu, Y.; Tan, Y.; Fu, Q.; Lin, M.; He, J.; He, S.; Yang, M.; Chen, S.; Zhou, J. Reciprocating-flowing on-a-chip enables ultra-fast immunobinding for multiplexed rapid ELISA detection of SARS-CoV-2 antibody. *Biosens. Bioelectron.* **2021**, *176*, 112920. [[CrossRef](#)] [[PubMed](#)]
65. Hosokawa, K. Biomarker Analysis on a Power-free Microfluidic Chip Driven by Degassed Poly(dimethylsiloxane). *Anal. Sci.* **2021**, *37*, 399–406. [[CrossRef](#)] [[PubMed](#)]

66. Tsagkaris, A.S.; Migliorelli, D.; Uttl, L.; Filippini, D.; Pulkrabova, J.; Hajslova, J. A microfluidic paper-based analytical device (muPAD) with smartphone readout for chlorpyrifos-oxon screening in human serum. *Talanta* **2021**, *222*, 121535. [[CrossRef](#)]
67. Li, X.; Zhang, X.; Liu, Q.; Zhao, W.; Liu, S.; Sui, G. Microfluidic System for Rapid Detection of Airborne Pathogenic Fungal Spores. *ACS Sens.* **2018**, *3*, 2095–2103. [[CrossRef](#)]
68. Hong, S.C.; Kang, J.S.; Lee, J.E.; Kim, S.S.; Jung, J.H. Continuous aerosol size separator using inertial microfluidics and its application to airborne bacteria and viruses. *Lab Chip* **2015**, *15*, 1889–1897. [[CrossRef](#)]
69. Ma, Z.; Zheng, Y.; Cheng, Y.; Xie, S.; Ye, X.; Yao, M. Development of an integrated microfluidic electrostatic sampler for bioaerosol. *J. Aerosol Sci.* **2016**, *95*, 84–94. [[CrossRef](#)]
70. Jing, W.; Jiang, X.; Zhao, W.; Liu, S.; Cheng, X.; Sui, G. Microfluidic Platform for Direct Capture and Analysis of Airborne Mycobacterium tuberculosis. *Anal. Chem.* **2014**, *86*, 5815–5821. [[CrossRef](#)]
71. Choi, J.; Hong, S.C.; Kim, W.; Jung, J.H. Highly Enriched, Controllable, Continuous Aerosol Sampling Using Inertial Microfluidics and Its Application to Real-Time Detection of Airborne Bacteria. *ACS Sens.* **2017**, *2*, 513–521. [[CrossRef](#)]
72. Liu, Q.; Zhang, X.; Yao, Y.; Jing, W.; Liu, S.; Sui, G. A novel microfluidic module for rapid detection of airborne and waterborne pathogens. *Sens. Actuators B Chem.* **2018**, *258*, 1138–1145. [[CrossRef](#)]
73. Nasrabadi, A.M.; Park, J.-W.; Kim, H.S.; Han, J.S.; Hyun, J.; Yong, D.; Hwang, J. Assessment of indoor bioaerosols using a lab-made virtual impactor. *Aerosol Sci. Technol.* **2016**, *51*, 159–167. [[CrossRef](#)]
74. Yuan, H.; Zhang, D.; Shi, Y.; Li, B.; Yang, J.; Yu, X.; Chen, N.; Kakikawa, M. Cell concentration, viability and culture composition of airborne bacteria during a dust event in Beijing. *J. Environ. Sci.* **2017**, *55*, 33–40. [[CrossRef](#)]
75. Huang, H.-L.; Lee, M.-K.; Shih, H.-W. Assessment of Indoor Bioaerosols in Public Spaces by Real-Time Measured Airborne Particles. *Aerosol Air Qual. Res.* **2017**, *17*, 2276–2288. [[CrossRef](#)]
76. Hsiao, P.-K.; Cheng, C.-C.; Chang, K.-C.; Yiin, L.-M.; Hsieh, C.-J.; Tseng, C.-C. Performance of CHROMagar VRE Medium for the Detection of Airborne Vancomycin-Resistant/Sensitive *Enterococcus* Species. *Aerosol Sci. Technol.* **2013**, *48*, 173–183. [[CrossRef](#)]
77. Mirhoseini, S.H.; Nikaeen, M.; Satoh, K.; Makimura, K. Assessment of Airborne Particles in Indoor Environments: Applicability of Particle Counting for Prediction of Bioaerosol Concentrations. *Aerosol Air Qual. Res.* **2016**, *16*, 1903–1910. [[CrossRef](#)]
78. Duquenne, P. On the Identification of Culturable Microorganisms for the Assessment of Biodiversity in Bioaerosols. *Ann. Work. Expo. Health* **2017**, *62*, 139–146. [[CrossRef](#)] [[PubMed](#)]
79. Jäckel, U.; Martin, E.; Schäfer, J. Heterogeneity in Cultivation-Based Monitoring of Airborne Bacterial Biodiversity in Animal Farms. *Ann. Work. Expo. Health* **2017**, *61*, 643–655. [[CrossRef](#)]
80. Schäfer, J.; Weiß, S.; Jäckel, U. Preliminary Validation of a Method Combining Cultivation and Cloning-Based Approaches to Monitor Airborne Bacteria. *Ann. Work. Expo. Health* **2017**, *61*, 633–642. [[CrossRef](#)] [[PubMed](#)]
81. Blais-Lecours, P.; Perrott, P.; Duchaine, C. Non-culturable bioaerosols in indoor settings: Impact on health and molecular approaches for detection. *Atmos. Environ.* **2015**, *110*, 45–53. [[CrossRef](#)] [[PubMed](#)]
82. Mbareche, H.; Veillette, M.; Bilodeau, G.J.; Duchaine, C. Fungal aerosols at dairy farms using molecular and culture techniques. *Sci. Total Environ.* **2019**, *653*, 253–263. [[CrossRef](#)]
83. Unterwurzacher, V.; Pogner, C.; Berger, H.; Strauss, J.; Strauss-Goller, S.; Gorfer, M. Validation of a quantitative PCR based detection system for indoor mold exposure assessment in bioaerosols. *Environ. Sci. Process. Impacts* **2018**, *20*, 1454–1468. [[CrossRef](#)]
84. Gaviria-Figueroa, A.; Preisner, E.C.; Hoque, S.; Feigley, C.E.; Norman, R.S. Emission and dispersal of antibiotic resistance genes through bioaerosols generated during the treatment of municipal sewage. *Sci. Total. Environ.* **2019**, *686*, 402–412. [[CrossRef](#)] [[PubMed](#)]
85. Uhrbrand, K.; Koponen, I.K.; Schultz, A.C.; Madsen, A.M. Evaluation of air samplers and filter materials for collection and recovery of airborne norovirus. *J. Appl. Microbiol.* **2018**, *124*, 990–1000. [[CrossRef](#)]
86. Coleman, K.K.; Sigler, W.V. Airborne Influenza A Virus Exposure in an Elementary School. *Sci. Rep.* **2020**, *10*, 1–7. [[CrossRef](#)]
87. Allegra, S.; Riffard, S.; Leclerc, L.; Girardot, F.; Stauffert, M.; Forest, V.; Pourchez, J. A valuable experimental setup to model exposure to Legionella's aerosols generated by shower-like systems. *Water Res.* **2020**, *172*, 115496. [[CrossRef](#)]
88. Anderson, B.D.; Yondon, M.; Bailey, E.S.; Duman, E.K.; Simmons, R.A.; Greer, A.G.; Gray, G.C. Environmental bioaerosol surveillance as an early warning system for pathogen detection in North Carolina swine farms: A pilot study. *Transbound. Emerg. Dis.* **2021**, *68*, 361–367. [[CrossRef](#)] [[PubMed](#)]
89. Orlofsky, E.; Benami, M.; Gross, A.; Dutt, M.; Gillor, O. Rapid MPN-Qpcr Screening for Pathogens in Air, Soil, Water, and Agricultural Produce. *Water, Air Soil Pollut.* **2015**, *226*, 1–10. [[CrossRef](#)]
90. Santos, R.; Sau, N.; Certucha, M.; Almendáriz, F.; Monge, A.; Zepeda, I.; Hernández, L. Rapid detection of bacteria, *Enterococcus faecalis*, in airborne particles of Hermosillo, Sonora, México. *J. Environ. Biol.* **2019**, *40*, 619–625. [[CrossRef](#)]
91. Yin, H.; Wu, Z.; Shi, N.; Qi, Y.; Jian, X.; Zhou, L.; Tong, Y.; Cheng, Z.; Zhao, J.; Mao, H. Ultrafast multiplexed detection of SARS-CoV-2 RNA using a rapid droplet digital PCR system. *Biosens. Bioelectron.* **2021**, *188*, 113282. [[CrossRef](#)]
92. Aoki, K.; Takai, K.; Nagasawa, T.; Kashiwagi, K.; Mori, N.; Matsubayashi, K.; Satake, M.; Tanaka, I.; Kodama, N.; Shimodaira, T.; et al. Combination of a SARS-CoV-2 IgG Assay and RT-PCR for Improved COVID-19 Diagnosis. *Ann. Lab. Med.* **2021**, *41*, 568–576. [[CrossRef](#)]
93. Liu, Q.; Zhang, X.; Li, X.; Liu, S.; Sui, G. A semi-quantitative method for point-of-care assessments of specific pathogenic bioaerosols using a portable microfluidics-based device. *J. Aerosol Sci.* **2018**, *115*, 173–180. [[CrossRef](#)]

94. Kwon, K.; Park, J.-W.; Hyun, K.-A.; Kwak, B.S.; Yong, D.E.; Hwang, J.; Jung, H.-I. Continuous adsorption and photothermal lysis of airborne bacteria using a gold-nanoparticle-embedded-geometrically activated surface interaction (gold-GASI) chip. *Sens. Actuators B Chem.* **2017**, *248*, 580–588. [[CrossRef](#)]
95. Qiu, G.; Gai, Z.; Saleh, L.; Tang, J.; Gui, T.; Kullak-Ublick, G.A.; Wang, J. Thermoplasmonic-Assisted Cyclic Cleavage Amplification for Self-Validating Plasmonic Detection of SARS-CoV-2. *ACS Nano* **2021**, *15*, 7536–7546. [[CrossRef](#)]
96. Cherkaoui, D.; Huang, D.; Miller, B.S.; Turbe, V.; McKendry, R.A. Harnessing recombinase polymerase amplification for rapid multi-gene detection of SARS-CoV-2 in resource-limited settings. *Biosens. Bioelectron.* **2021**, *189*, 113328. [[CrossRef](#)] [[PubMed](#)]
97. He, Y.; Xie, T.; Tong, Y. Rapid and highly sensitive one-tube colorimetric RT-LAMP assay for visual detection of SARS-CoV-2 RNA. *Biosens. Bioelectron.* **2021**, *187*, 113330. [[CrossRef](#)]
98. Yin, K.; Ding, X.; Xu, Z.; Li, Z.; Wang, X.; Zhao, H.; Otis, C.; Li, B.; Liu, C. Multiplexed colorimetric detection of SARS-CoV-2 and other pathogens in wastewater on a 3D printed integrated microfluidic chip. *Sens. Actuators B Chem.* **2021**, *344*, 130242. [[CrossRef](#)]
99. King, M.D.; Lacey, R.E.; Pak, H.; Fearing, A.; Ramos, G.; Baig, T.; Smith, B.; Koustova, A. Assays and enumeration of bioaerosols—traditional approaches to modern practices. *Aerosol Sci. Technol.* **2020**, *54*, 611–633. [[CrossRef](#)]
100. Bonifait, L.; Veillette, M.; Létourneau, V.; Grenier, D.; Duchaine, C. Detection of *Streptococcus suis* in Bioaerosols of Swine Confinement Buildings. *Appl. Environ. Microbiol.* **2014**, *80*, 3296–3304. [[CrossRef](#)]
101. Chang, C.-W.; Lin, M.-H.; Huang, S.-H.; Hornig, Y.-J. Parameters affecting recoveries of viable *Staphylococcus aureus* bioaerosols in liquid-based samplers. *J. Aerosol Sci.* **2019**, *136*, 82–90. [[CrossRef](#)]
102. Chang, C.-W.; Hung, N.-T.; Chen, N.-T. Optimization and application of propidium monoazide-quantitative PCR method for viable bacterial bioaerosols. *J. Aerosol Sci.* **2017**, *104*, 90–99. [[CrossRef](#)]
103. Fronczek, C.F.; Yoon, J.-Y. Biosensors for Monitoring Airborne Pathogens. *J. Lab. Autom.* **2015**, *20*, 390–410. [[CrossRef](#)] [[PubMed](#)]
104. Langer, V.; Hartmann, G.; Niessner, R.; Seidel, M. Rapid quantification of bioaerosols containing *L. pneumophila* by Coriolis® μ air sampler and chemiluminescence antibody microarrays. *J. Aerosol Sci.* **2012**, *48*, 46–55. [[CrossRef](#)]
105. Yoo, M.S.; Shin, M.; Kim, Y.; Jang, M.; Choi, Y.E.; Park, S.J.; Choi, J.; Lee, J.; Park, C. Development of electrochemical biosensor for detection of pathogenic microorganism in Asian dust events. *Chemosphere* **2017**, *175*, 269–274. [[CrossRef](#)]
106. Kim, J.; Jin, J.-H.; Kim, H.S.; Song, W.; Shin, S.-K.; Yi, H.; Jang, D.-H.; Shin, S.; Lee, B.Y. Fully Automated Field-Deployable Bioaerosol Monitoring System Using Carbon Nanotube-Based Biosensors. *Environ. Sci. Technol.* **2016**, *50*, 5163–5171. [[CrossRef](#)]
107. Shen, F.; Tan, M.; Wang, Z.; Yao, M.; Xu, Z.; Wu, Y.; Wang, J.; Guo, X.; Zhu, T. Integrating Silicon Nanowire Field Effect Transistor, Microfluidics and Air Sampling Techniques For Real-Time Monitoring Biological Aerosols. *Environ. Sci. Technol.* **2011**, *45*, 7473–7480. [[CrossRef](#)]
108. Morris, D.R.; Fatisson, J.; Olsson, A.L.; Tufenkji, N.; Ferro, A.R. Real-time monitoring of airborne cat allergen using a QCM-based immunosensor. *Sens. Actuators B Chem.* **2014**, *190*, 851–857. [[CrossRef](#)]
109. Farka, Z.; Kovar, D.; Skládal, P. Quartz crystal microbalance biosensor for rapid detection of aerosolized microorganisms. In *Chemical, Biological, Radiological, Nuclear, and Explosives (CBRNE) Sensing XVI*; International Society for Optics and Photonics: Bellingham, WA, USA, 2015; Volume 9455, p. 945507. [[CrossRef](#)]
110. Kovar, D.; Farka, Z.; Skládal, P. Detection of Aerosolized Biological Agents Using the Piezoelectric Immunosensor. *Anal. Chem.* **2014**, *86*, 8680–8686. [[CrossRef](#)] [[PubMed](#)]
111. Toma, K.; Miki, D.; Kishikawa, C.; Yoshimura, N.; Miyajima, K.; Arakawa, T.; Yatsuda, H.; Mitsubayashi, K. Repetitive Immunoassay with a Surface Acoustic Wave Device and a Highly Stable Protein Monolayer for On-Site Monitoring of Airborne Dust Mite Allergens. *Anal. Chem.* **2015**, *87*, 10470–10474. [[CrossRef](#)] [[PubMed](#)]
112. Toma, K.; Harashima, Y.; Yoshimura, N.; Arakawa, T.; Yatsuda, H.; Kanamori, K.; Mitsubayashi, K. Semicontinuous Measurement of Mite Allergen (Der f 2) Using a Surface Acoustic Wave Immunosensor under Moderate pH for Long Sensor Lifetime. *Sens. Mater.* **2017**, *29*, 1679–1687.
113. Toma, K.; Miki, D.; Yoshimura, N.; Arakawa, T.; Yatsuda, H.; Mitsubayashi, K. A gold nanoparticle-assisted sensitive SAW (surface acoustic wave) immunosensor with a regeneratable surface for monitoring of dust mite allergens. *Sens. Actuators B Chem.* **2017**, *249*, 685–690. [[CrossRef](#)]
114. Toma, K.; Horibe, M.; Kishikawa, C.; Yoshimura, N.; Arakawa, T.; Yatsuda, H.; Shimomura, H.; Mitsubayashi, K. Rapid and repetitive immunoassay with a surface acoustic wave device for monitoring of dust mite allergens. *Sens. Actuators B Chem.* **2017**, *248*, 924–929. [[CrossRef](#)]
115. Toma, K.; Oishi, K.; Kato, M.; Kurata, K.; Yoshimura, N.; Arakawa, T.; Yatsuda, H.; Kanamori, K.; Mitsubayashi, K. Precipitate-enhanced SAW immunosensor for sensitive monitoring of mite allergens. *Sens. Actuators B Chem.* **2019**, *296*, 126579. [[CrossRef](#)]
116. Usachev, E.V.; Tam, A.M.; Usacheva, O.V.; Agranovski, I.E. The sensitivity of surface plasmon resonance based viral aerosol detection. *J. Aerosol Sci.* **2014**, *76*, 39–47. [[CrossRef](#)]
117. Usachev, E.V.; Agranovski, E.; Usacheva, O.V.; Agranovski, I.E. Multiplexed Surface Plasmon Resonance based real time viral aerosol detection. *J. Aerosol Sci.* **2015**, *90*, 136–143. [[CrossRef](#)]
118. Usachev, E.; Usacheva, O.; Agranovski, I. Surface plasmon resonance-based bacterial aerosol detection. *J. Appl. Microbiol.* **2014**, *117*, 1655–1662. [[CrossRef](#)]
119. Qiu, G.; Yue, Y.; Tang, J.; Zhao, Y.-B.; Wang, J. Total Bioaerosol Detection by a Succinimidyl-Ester-Functionalized Plasmonic Biosensor To Reveal Different Characteristics at Three Locations in Switzerland. *Environ. Sci. Technol.* **2019**, *54*, 1353–1362. [[CrossRef](#)]

120. Negron, A.; DeLeon-Rodriguez, N.; Waters, S.; Ziemba, L.D.; Anderson, B.; Bergin, M.; Konstantinidis, K.T.; Nenes, A. Using flow cytometry and light-induced fluorescence to characterize the variability and characteristics of bioaerosols in springtime in Metro Atlanta, Georgia. *Atmos. Chem. Phys. Discuss.* **2020**, *20*, 1817–1838. [[CrossRef](#)]
121. Feeney, P.; Fernández-Rodríguez, S.; Molina, R.; McGillicuddy, E.; Hellebust, S.; Quirke, M.; Daly, S.; ÓConnor, D.; Sodeau, J. A comparison of on-line and off-line bioaerosol measurements at a biowaste site. *Waste Manag.* **2018**, *76*, 323–338. [[CrossRef](#)]
122. Lu, C.; Zhang, P.; Wang, G.; Zhu, J.; Tang, X.; Huang, W.; Chen, S.; Xu, X.; Huang, H. Accurate measurement of airborne biological particle concentration based on laser-induced fluorescence technique. *J. Aerosol Sci.* **2018**, *117*, 24–33. [[CrossRef](#)]
123. Gaudiuso, R.; Melikechi, N.; Abdel-Salam, Z.A.; Harith, M.A.; Palleschi, V.; Motto-Ros, V.; Busser, B. Laser-induced breakdown spectroscopy for human and animal health: A review. *Spectrochim. Acta Part B At. Spectrosc.* **2019**, *152*, 123–148. [[CrossRef](#)]
124. Esquivel-Gonzalez, S.; Aizpuru, A.; Patrón-Soberano, A.; Arriaga, S. Characterization of bioaerosol emissions from two biofilters during treatment of toluene vapours using epifluorescence microscopy. *Int. Biodeterior. Biodegrad.* **2017**, *123*, 78–86. [[CrossRef](#)]
125. Chen, L.-W.A.; Zhang, M.; Liu, T.; Fortier, K.; Chow, J.C.; Alonzo, F.; Kolberg, R.; Cao, J.; Lin, G.; Patel, T.Y.; et al. Evaluation of epifluorescence methods for quantifying bioaerosols in fine and coarse particulate air pollution. *Atmos. Environ.* **2019**, *213*, 620–628. [[CrossRef](#)]
126. Nasir, Z.; Rolph, C.; Collins, S.; Stevenson, D.; Gladding, T.; Hayes, E.; Williams, B.; Khera, S.; Jackson, S.; Bennett, A.; et al. A Controlled Study on the Characterisation of Bioaerosols Emissions from Compost. *Atmosphere* **2018**, *9*, 379. [[CrossRef](#)]
127. Gong, Z.; Pan, Y.L.; Videen, G.; Wang, C. Optical trapping-Raman spectroscopy (OT-RS) with embedded microscopy imaging for concurrent characterization and monitoring of physical and chemical properties of single particles. *Anal. Chim. Acta* **2018**, *1020*, 86–94. [[CrossRef](#)]
128. Groulx, N.; Lecours, C.; Turgeon, N.; Volckens, J.; Tremblay, M.-E.; Duchaine, C. Nanoscale aerovirology: An efficient yet simple method to analyze the viral distribution of single bioaerosols. *Aerosol Sci. Technol.* **2016**, *50*, 732–739. [[CrossRef](#)]
129. Valsan, A.E.; Priyamvada, H.; Ravikrishna, R.; Després, V.R.; Biju, C.; Sahu, L.K.; Kumar, A.; Verma, R.; Philip, L.; Gunthe, S.S. Morphological characteristics of bioaerosols from contrasting locations in southern tropical India—A case study. *Atmos. Environ.* **2015**, *122*, 321–331. [[CrossRef](#)]
130. Park, J.-W.; Park, C.W.; Lee, S.H.; Hwang, J. Fast Monitoring of Indoor Bioaerosol Concentrations with ATP Bioluminescence Assay Using an Electrostatic Rod-Type Sampler. *PLoS ONE* **2015**, *10*, e0125251. [[CrossRef](#)]
131. Kim, H.R.; An, S.; Hwang, J.; Park, J.H.; Byeon, J.H. In situ lysis droplet supply to efficiently extract ATP from dust particles for near-real-time bioaerosol monitoring. *J. Hazard. Mater.* **2019**, *369*, 684–690. [[CrossRef](#)] [[PubMed](#)]
132. Nasrabadi, A.M.; Han, J.S.; Farid, M.M.; Lee, S.-G.; Hwang, J. Real-time separation of aerosolized *Staphylococcus epidermidis* and polystyrene latex particles with similar size distributions. *Aerosol Sci. Technol.* **2017**, *51*, 1389–1397. [[CrossRef](#)]
133. Bryan, N.C.; Christner, B.C.; Guzik, T.G.; Granger, D.J.; Stewart, M.F. Abundance and survival of microbial aerosols in the troposphere and stratosphere. *ISME J.* **2019**, *13*, 2789–2799. [[CrossRef](#)]
134. Hou, P.; Xu, Y.; Wang, H.; He, H. Detection of bovine viral diarrhoea virus genotype 1 in aerosol by a real time RT-PCR assay. *BMC Vet. Res.* **2020**, *16*, 1–9. [[CrossRef](#)]
135. Kim, S.-J.; Bae, P.K.; Choi, M.; Keem, J.O.; Chung, W.; Shin, Y.-B. Fabrication and Application of Levam–PVA Hydrogel for Effective Influenza Virus Capture. *ACS Appl. Mater. Interfaces* **2020**, *12*, 29103–29109. [[CrossRef](#)] [[PubMed](#)]
136. Miyajima, K.; Suzuki, Y.; Miki, D.; Arai, M.; Arakawa, T.; Shimomura, H.; Shiba, K.; Mitsubayashi, K. Direct analysis of airborne mite allergen (Der f1) in the residential atmosphere by chemifluorescent immunoassay using bioaerosol sampler. *Talanta* **2014**, *123*, 241–246. [[CrossRef](#)]
137. Skladal, P.; Svabenska, E.; Žeravík, J.; Pribyl, J.; Šišková, P.; Tjarnhage, T.; Gustafson, I. Electrochemical Immunosensor Coupled to Cyclone Air Sampler for Detection of *Escherichia coli* DH5 α in Bioaerosols. *Electroanalysis* **2011**, *24*, 539–546. [[CrossRef](#)]
138. Rahmani, A.R.; Leili, M.; Azarian, G.; Poormohammadi, A. Sampling and detection of corona viruses in air: A mini review. *Sci. Total. Environ.* **2020**, *740*, 140207. [[CrossRef](#)] [[PubMed](#)]